Detailed measurements of Ide transformer devices

Horst Eckardt[1], Bernhard Foltz[2], Karlheinz Mayer[3]
A.I.A.S. and UPITEC
(www.aias.us, www.atomicprecision.com, www.upitec.org)

July 16, 2017

Abstract

The energy generator device of Osamu Ide has been replicated in several variants. This device is a transformer driven by rectangular high-frequency pulses and therefore can only be understood within the framework of high-frequency engineering. After the Munich group had tested the original device of Ide and had successfully replicated the effects, intensive measurements were performed with three additional transformer constructs and variants of the circuitry. The placement of data extraction points was improved. Various measurements of input and output power have been carried out. As a result, the parameter ranges for overunity operation (where measured output power exceeds measured input power) could be determined. The input power turned out to be negative over wide frequency ranges. An explanation for this behaviour is given.

Keywords: transformer; power measurement; high-frequency measurement; spacetime energy.

1 Introduction

The Munich group has replicated the experiments of Osamu Ide in several stages. Ide has shown that there is an additional non-classical current contribution when a transformer is driven by a pulse of DC [1]- [3]. The Munich group was able to reproduce this experiment practically [6]. In addition, the AIAS institute was able to explain this behaviour by an adopted theory [5], based on the general unified ECE field theory [7]. It was also shown that the oscillatory behaviour at the switch-on pulse can be modeled by a variation of the inductance value of the transformer [6]. So far the experiments of the Munich group had been based on Ide papers [1] and [2] in order to replicate the basic effects. In this article we extend our investigations to the device configuration given in [3]. Two rectifiers have been added to drive a real load consisting of ohmic resistances. This avoids objections against transient effects in load measurements, the power is dissipated thermally by an ohmic load. The dynamic power measurement from AC currents is restricted to the input side.

[1]email: mail@horst-eckardt.de
[2]email: mail@bernhard-foltz.de
[3]email: k.mayer@spirit-of-matter.de

In this work we observed a negative input power over wide parameter regions. This was also observed partially by Ide in his measurements. We will discuss to which extent this can be attributed to a back-flow of energy to the power source. It will be shown that the Ide device can be understood in its classical parts as a high-frequency device. Nevertheless, overunity-effects (where measured output power exceeds measured input power) are clearly visible.

2 Circuit design

The principal circuit layout of the device used is graphed in Fig. 1. The transformer is driven with a rectangular voltage generated by a MOSFET which is triggered by a digital pulse generator. This generator was constructed specifically for this purpose and was already described in [6]. A shunt resistor R_1 was used to measure the input current. In the original measurements [6], this resistor was placed at the point denoted by the dashed lines (as it originally was by Ide). The coil wires are wound with primary and secondary lines in parallel, leading to a capacitive feedback between primary and secondary site. This capacitive coupling is much higher than in a conventional transformer with separated windings (see section 3). Therefore the input power has to be measured outside possible feedback loops in the circuit and the shunt was placed now where indicated. The (time-dependent) input current then is

$$I(t) = \frac{U_1(t)}{R_1} \tag{1}$$

and the input power is integrated in the oscilloscope by evaluating

$$P_{in} = \frac{1}{T} \int_0^T U_0(t)\, I(t)\, dt \tag{2}$$

where U_0 is the input voltage, U_1 is the voltage measured at R_1 and T is the period of the pulsed input signal. The input voltage should be constant but this is not always the case due to backward interaction of the sharp pulses to the power source (even if a DC battery is used).

At the secondary site, a two-fold rectifier was deployed as used by Ide in [3]. Positive and negative half-waves are rectified separately. This is more effective than using a bridge rectifier as will be shown in the next section. Both rectifiers can be operated independently by switches. The output power is consumed at the load resistances R_2. Since these resistances are fed with DC voltages, the output power can safely be computed by

$$P_{out} = \frac{U^2}{R_2} \tag{3}$$

where U is the voltage measured at R_2. This computation was done separately for both rectifier branches. A coupling capacitor C_1 between primary and secondary side was used optionally as described in the next section.

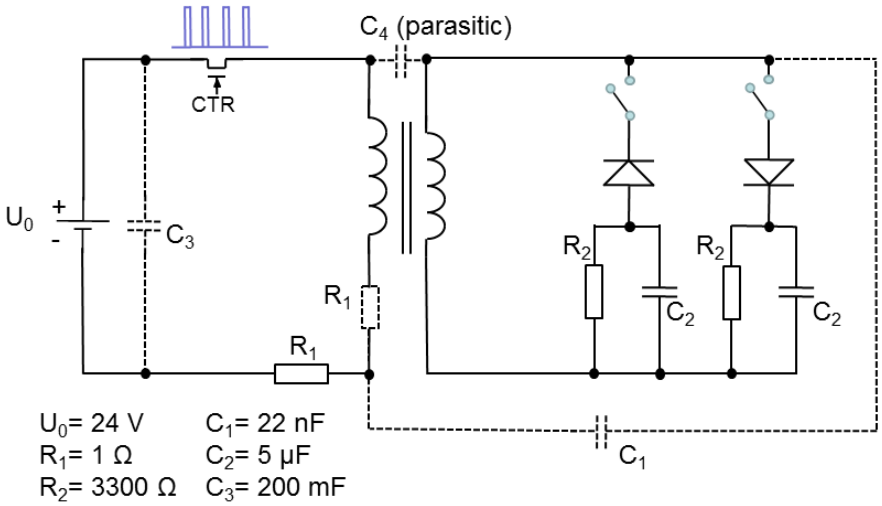

Figure 1: Circuit for the transformer tests.

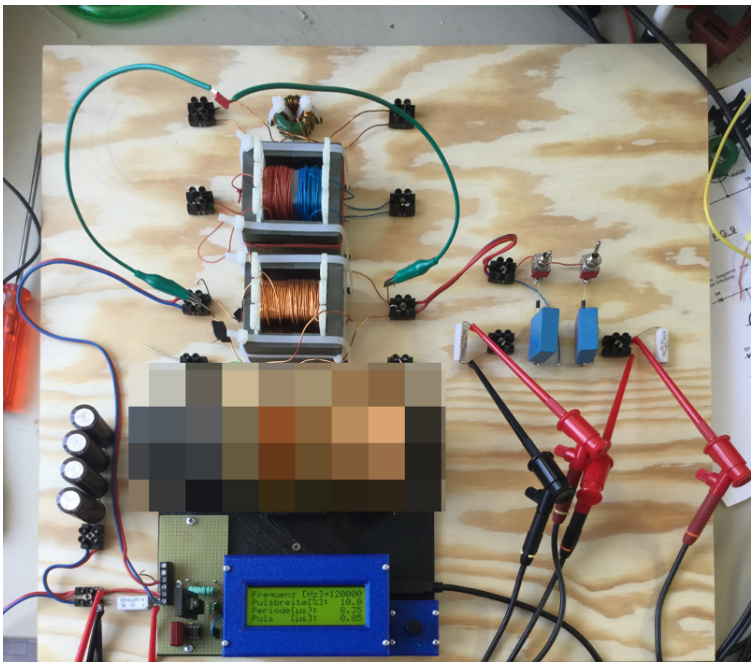

Figure 2: Test setup.

3 Results

A test setup has been constructed as shown in Fig. 2 (some confidential details have been pixelated). Three transformers were used for comparison: two E-I-cores and one torus core. The microprocessor-based frequency generator is at

the bottom, the rectifiers are at the right. The coils are denoted coil 3-5 for internal reasons. Cores of no. 3 and 4 are from N87 material of TDK, no. 5 is a small choke coil. Input voltage was always 24 V DC. The device parameters (including the parasitic capacitance C_4 between primary/secondary windings) are listed in Table 1. There was no measurable value of C_4 for coil 4 because primary and secondary windings were separated in that device.

device	no. of windings	geometry	inductance	capacitance C_4
coil 3	35	E-I core	0.88 mH	730 nF
coil 4	35	E-I core	0.67 mH	-
coil 5	7	torus	0.75 mH	27 pF

Table 1: Transformer device parameters.

3.1 Coil 3

Measurements were carried out first without capacitors C_1 and C_3 in Fig. 1. The frequency dependencies of P_{in} and P_{out} according to Eqs. (2) and (3) are graphed in Figs. 3-5. The input power is negative over large frequency ranges. A 4-channel differential oscilloscope of TiePie was used for measurements. Usage of another oscilloscope gave similar results so negative input power seems not to be an artifact of measuring. In some cases the differential oscilloscope had problems with adjusting the zero point of channels so that a shift of a few milliamperes in the measured input current may be present. This does however not invalidate the principal overunity measurements. This was one reason why we did not compute the COP (ratio between output and input power) but showed the power difference directly in the diagrams.

Using only the negative half-wave (Fig. 3), leads to larger output power than input power, even when considering only the absolute values, over larger frequency ranges. This means overunity measurement. For the positive half-wave rectifier (Fig. 4) there is no overunity behaviour and power values are all positive. When both rectifiers are operated together, both input and output power increase, but the result remains in underunity range (Fig. 5). The reason for this behaviour is the asymmetric signal produced by the falling edge of input voltage as discussed later. Consequently, a bridge rectifier would give similar results as using both half-wave rectifiers. The results are summarized in Fig. 6 where the differences between output and input power are graphed. A positive value means overunity measurement while negative values denote conventional behaviour with power loss.

The capacitor C_1 was originally introduced to simulate a capacitive coupling between primary and secondary windings of coil 4, where no such coupling exists otherwise (see Table 1). Here we used it for coil 3 to obtain an enhanced coupling. The capacitor C_3 was added for smoothing out the input voltage and for being a reservoir of energy eventually being passed back to the voltage source.

When capacitors C_1 and C_3 are added, we have a two-fold effect: There is a backward coupling from secondary to primary site by C_1 and the input voltage is greatly stabilized by C_3. The power measurements are shown in Fig. 7 and their difference is graphed in Fig. 8. In the high-frequency limit the efficiency is

very low due to strongly rising input power. The lower frequency range below 140 kHz may be compared to Fig. 3, both for the negative half-wave rectifier. The range of negative power is reduced, and a maximum of both input and output at about 80 kHz is visible.

The reason for negative input power display has been investigated in Fig. 9. The signals of input voltage at the primary side (green), the input current (blue-green) and input power (red) have been resolved in detail, with frequency 200 kHz, without capacitor C_3 but with coupling capacitor C_1. It can be seen that there is a significant impact of the input current on the input voltage that should remain constant ideally. There is a phase shift of 180 degrees between input current and voltage, leading to the time-resolved power (red signal). It can be seen that the negative parts of the wave overbalance the positive parts when the signal is integrated. For these reasons the averaged power value is negative. This effect is strongly reduced as soon as capacitor C_3 is added.

The oscillations are characteristic for the Ide device, caused by the rectangular excitation signal. The oscillatory behaviour of the transformer has been analyzed in Figs. 10 and 11. Both are recorded at 15 kHz, showing input voltage (green), voltage at the primary side of the coil (blue) and the input current (blue-green). The duty cycle of the rectangular signal is 15% (as in all measurements if not indicated differently). This range is visible as a positive rectangular voltage at the coil, where the current increases nearly linearly. After switching off the input voltage, there is a negative switch-off peak at the coil as expected, followed by a negative pulse being somewhat longer than the (positive) duty cycle. This is the reason why the rectifier for the negative half-waves gives a higher power than that for the positive half-waves. The negative peak can reach -60 V in extremal cases. After that, a sinusoidal oscillation occurs with a frequency of 211 kHz. This is an eigen resonance of the core material, appearing as a damped wave.

The eigen resonance changes if the coupling capacitor C_1 is added to the circuit, see Fig. 11. The eigen frequency goes significantly down to 140 kHz because the capacity in the internal oscillator has increased. There is also an effect on the fast oscillatory behaviour of the input current during on-time (duty cycle). Without coupling capacitor, the current oscillates at about 5 MHz, after switch-off at about 3.6 MHz. With coupling capacitor added, these values change to about 3.7 MHz and 3 - 6 MHz. These fast oscillations represent the “ringing” of the transformer while the low-frequency oscillations have no classical counterpart in an ordinary transformer.

As a last result for coil 3 we present the same measuremts as in Figs. 7 ane 8, here for the low-frequency range <30 kHz, with both capacitors C_1 and C_3. An overunity behaviour can be observed above 3.5 kHz in Fig. 12, also well visible in the power difference diagram Fig. 13. The output voltage at the rectifier (negative half-wave) is graphed in Fig. 14, revealing that this voltage is largest (in absolute values) at small frequencies. This means that the highest load (for effectively extracting power) can be applied in this range.

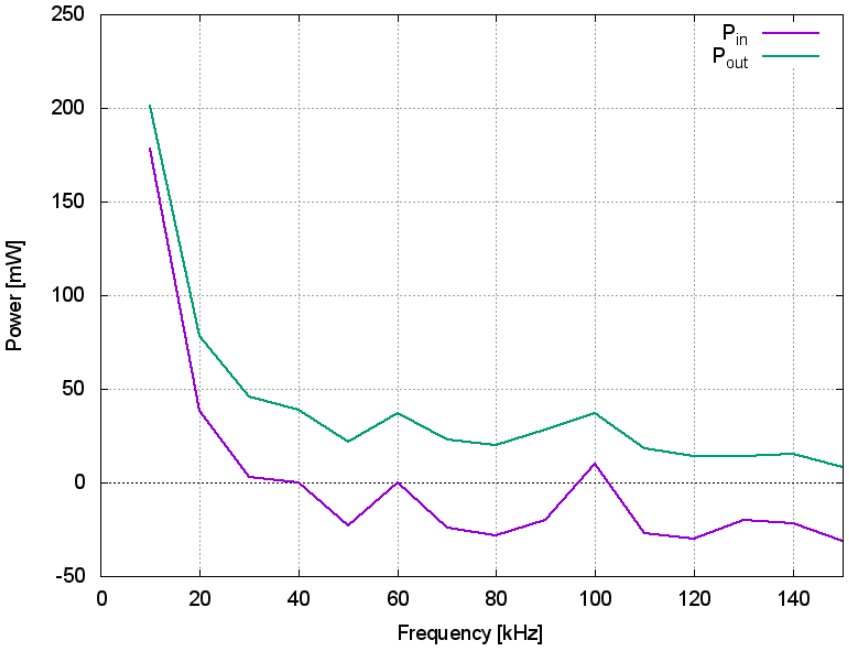

Figure 3: Input and output power of coil 3, neg. half-wave.

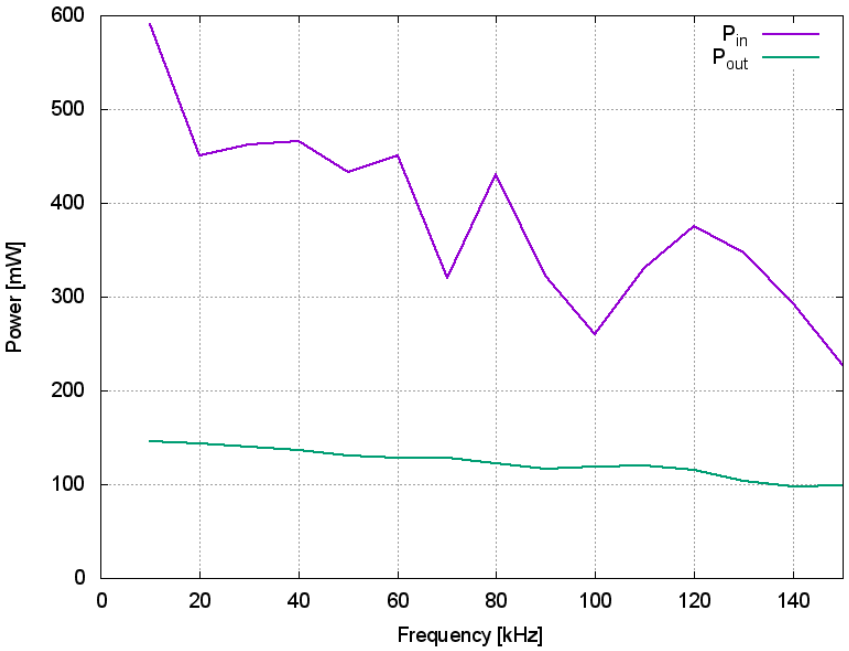

Figure 4: Input and output power of coil 3, pos. half-wave.

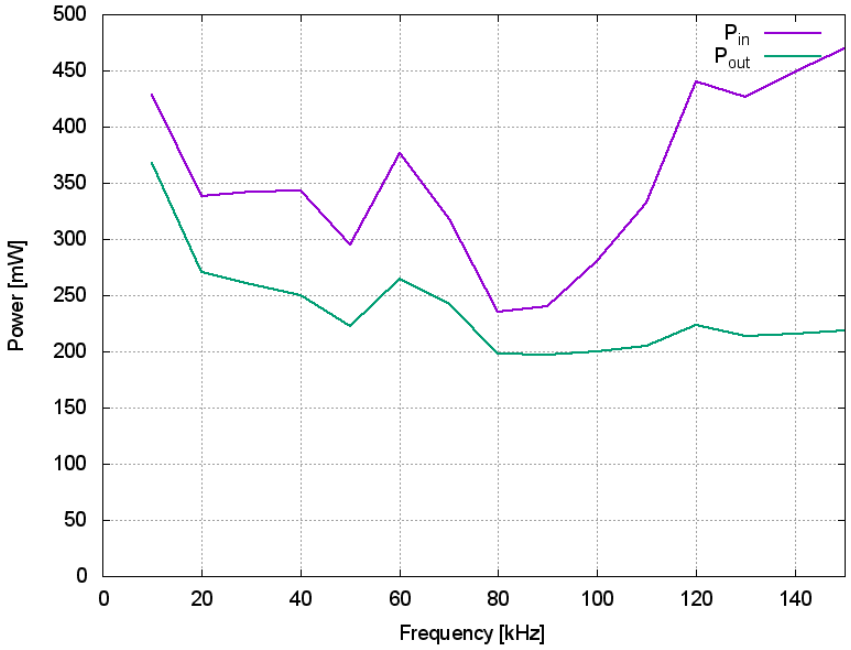

Figure 5: Input and output power of coil 3, both half-waves.

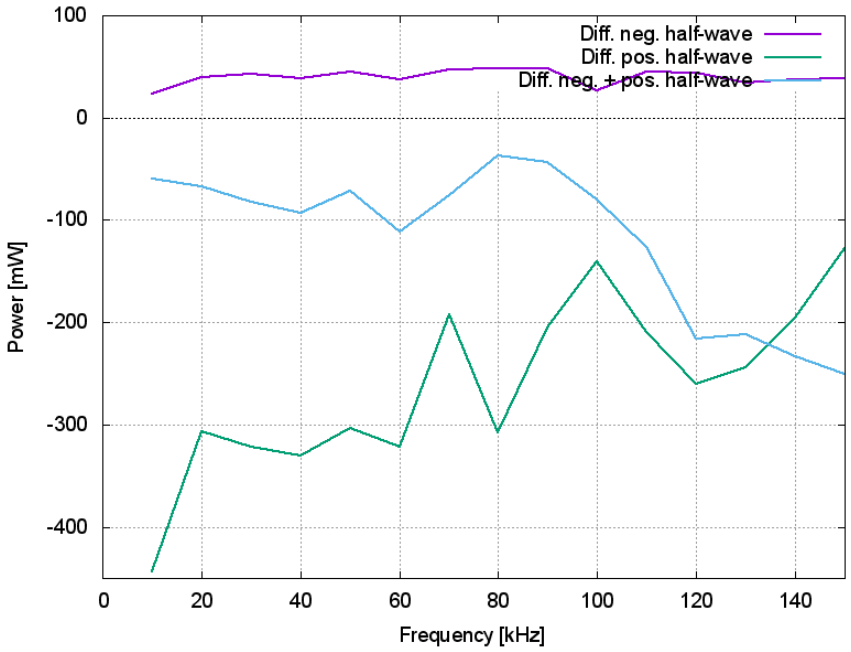

Figure 6: Power differences $P_{out} - P_{in}$.

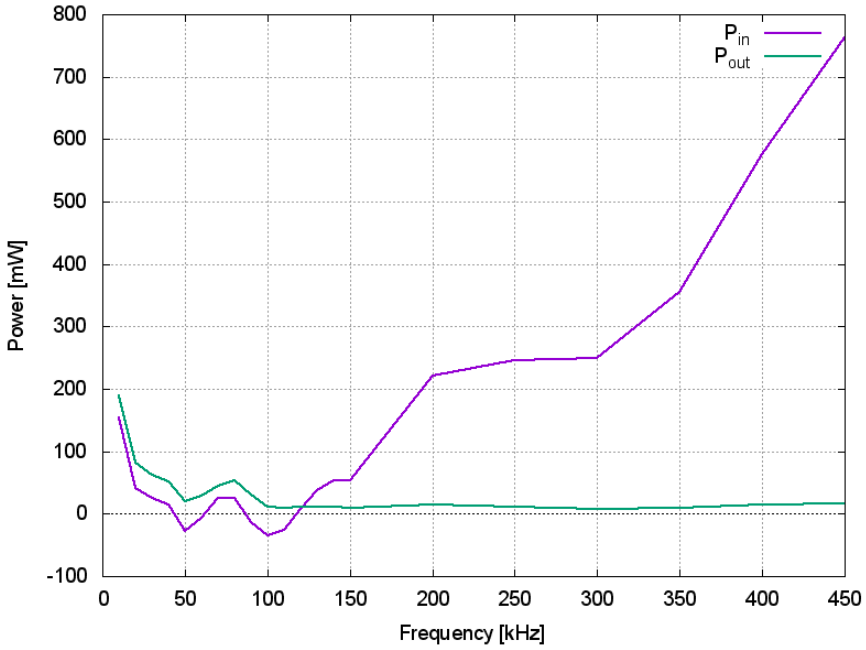

Figure 7: Input and output power of coil 3, with capacitors C_1 and C_3, neg. half-wave.

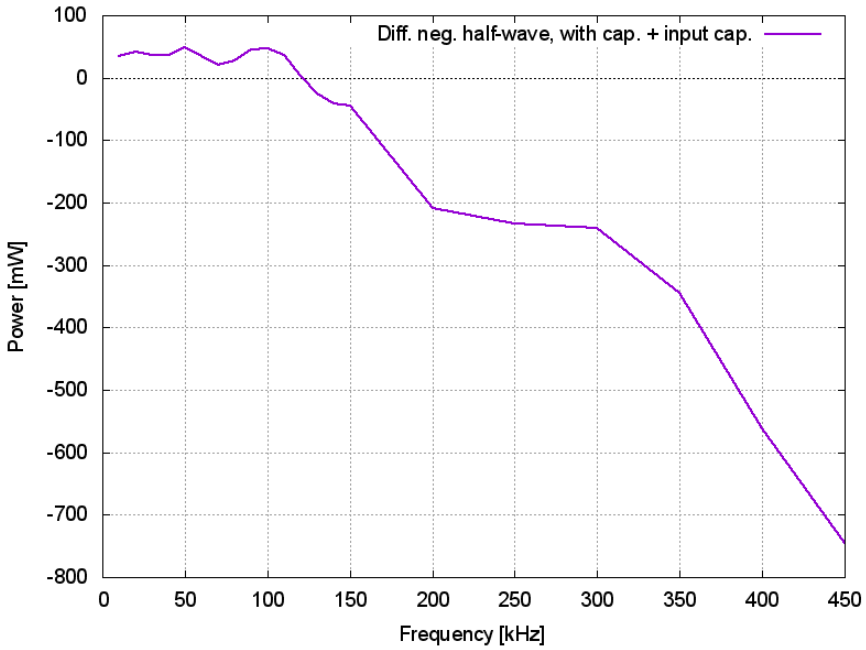

Figure 8: Power differences of Fig 7.

Figure 9: Time-resolved signals for input voltage (green), current (blue-green) and power (red).

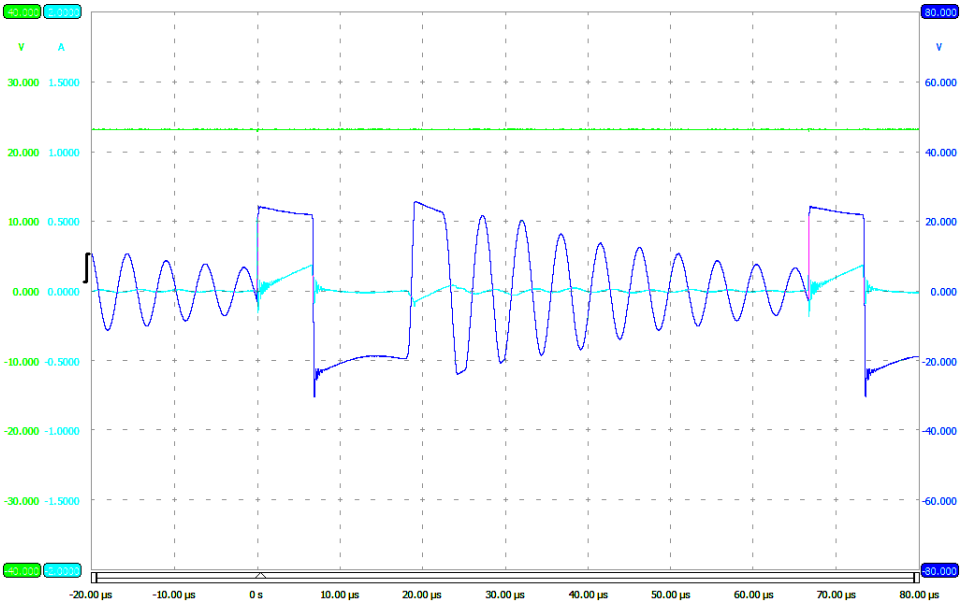

Figure 10: Time-resolved input voltage (green), input current (blue-green) and voltage at primary site (blue) at 15 kHz, without C_1.

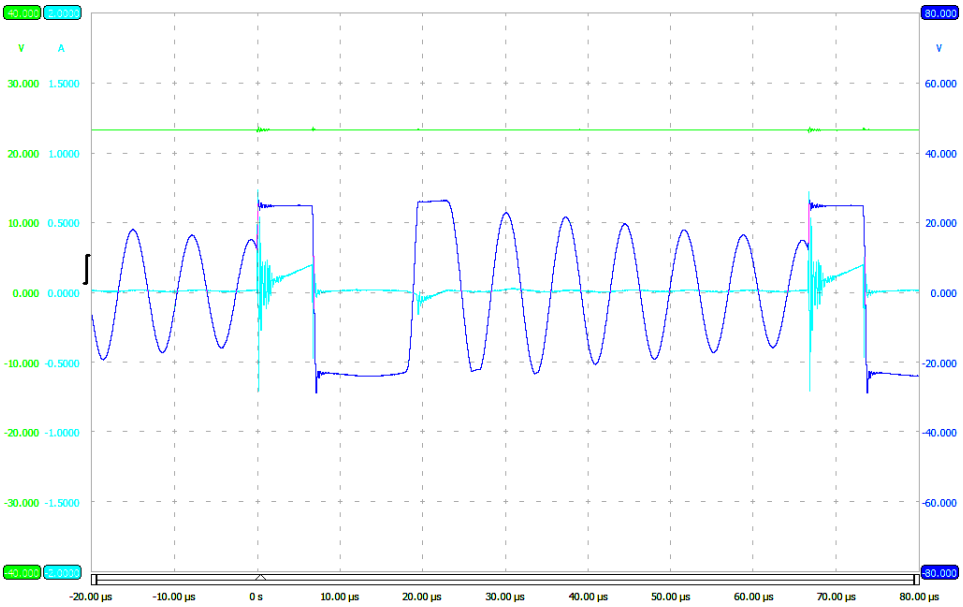

Figure 11: Time-resolved input voltage (green), input current (blue-green) and voltage at primary site (blue) at 15 kHz, with C_1.

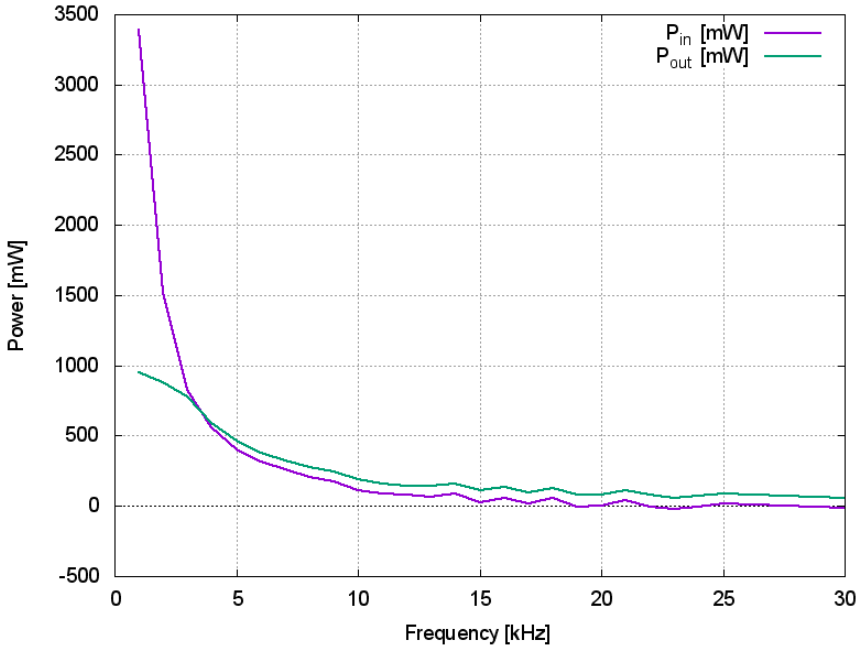

Figure 12: Input and output power of coil 3, low-frequency range.

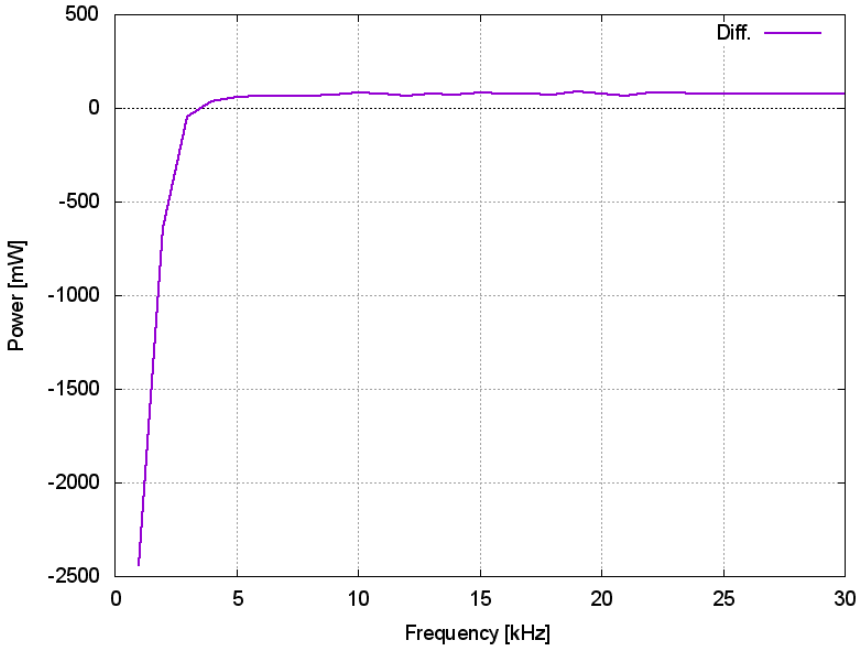

Figure 13: Power difference of Fig. 12, low-frequency range.

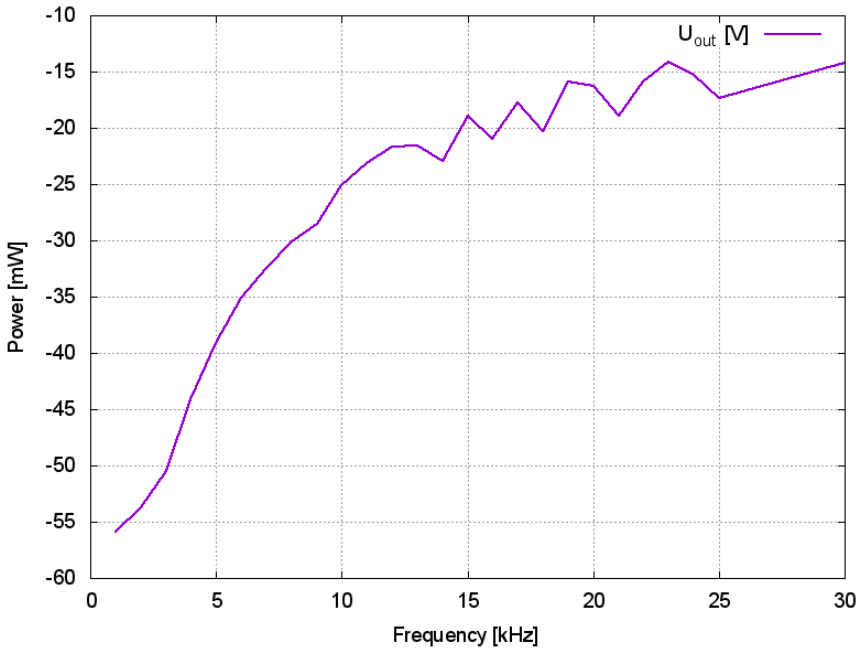

Figure 14: Output voltage (negative rectifier) in low-frequency range.

3.2 Coil 4

The same measurements as for coil 3 have been repeated for coil 4 which is identical to coil 3 except that the primary and secondary windings have been separated on the core. There are no primary and secondary wires conducted in parallel. The power results for the negative half-wave with capacitors C_1 and C_3 are graphed in Figs. 15 and 16, the output voltage at the rectifier is shown in Fig. 17. There is a similar behaviour found as for coil 3, but the overunity range starts at higher frequencies (>20 kHz).

A difference is found in the eigen oscillations. Fig. 18 shows the oscillations in the case without load (no rectifiers active). There are two frequencies: the eigen oscillation is about 231-237 kHz, and the "ringing oscillation"' takes longer in time, having been reduced to 980-1020 kHz, compared to several MHz in coil 3. There is no second rectangular signal part. This occurs when a load (negative rectifier) is added (Fig. 19). However there is a third frequency, appearing where a constant negative signal was in coil 3 directly after switching off the duty cycle. The frequency of this additional oscillation is at 549-561 kHz, lying between both other frequencies that are identical to those of Fig. 18.

As a last test we reduced the pulse frequency from 15 kHz to 8 kHz (Fig. 20). This is an unstable state where the current jumps between two states some times per second. In one state (this is shown in the Fig. 20) the current has a negative mean value of −30 mA. The current stays at this values where the core-induced oscillations fade away. This is quite unusual.

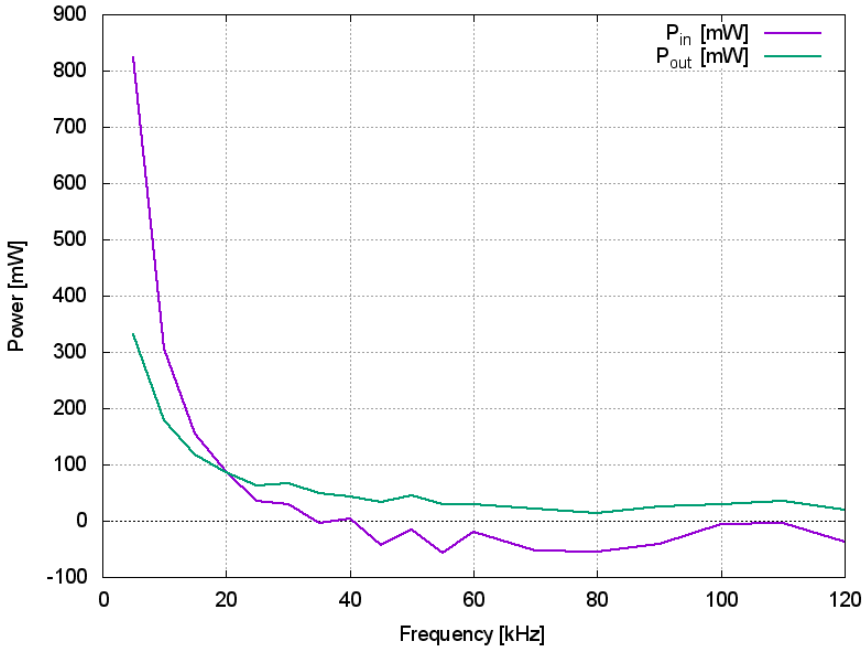

Figure 15: Input and output power of coil 4, neg. half-wave.

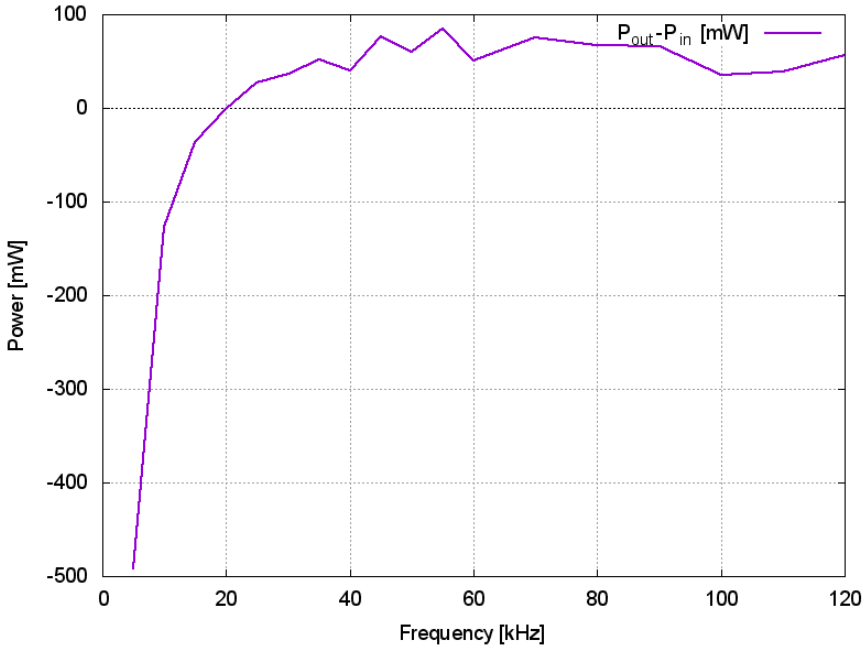

Figure 16: Power differences of coil 4 from Fig. 15.

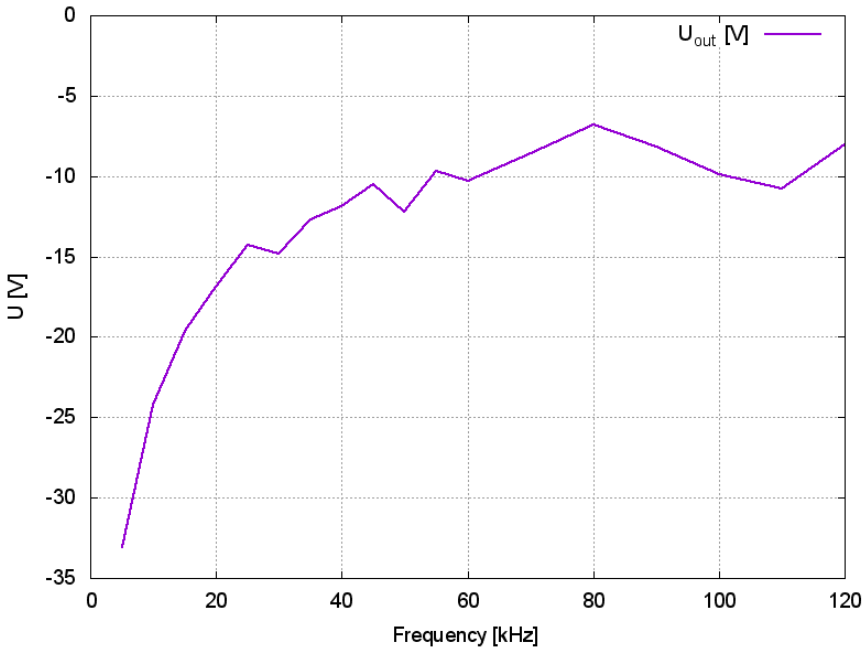

Figure 17: Output voltage (negative rectifier) of coil 4.

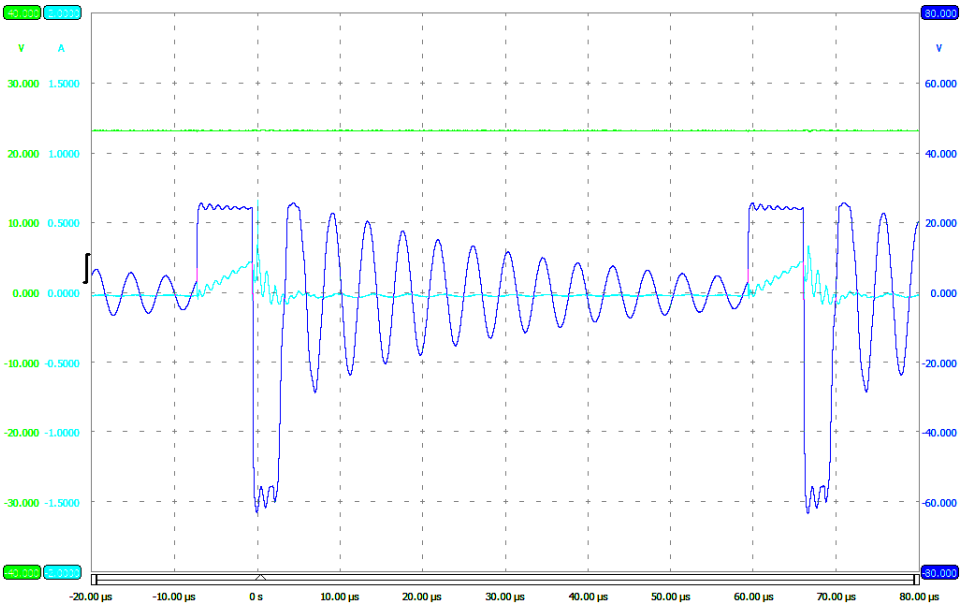

Figure 18: Time-resolved signals at 15 kHz for input voltage (green), current (blue-green) and power (blue), coil 4, no secondary load

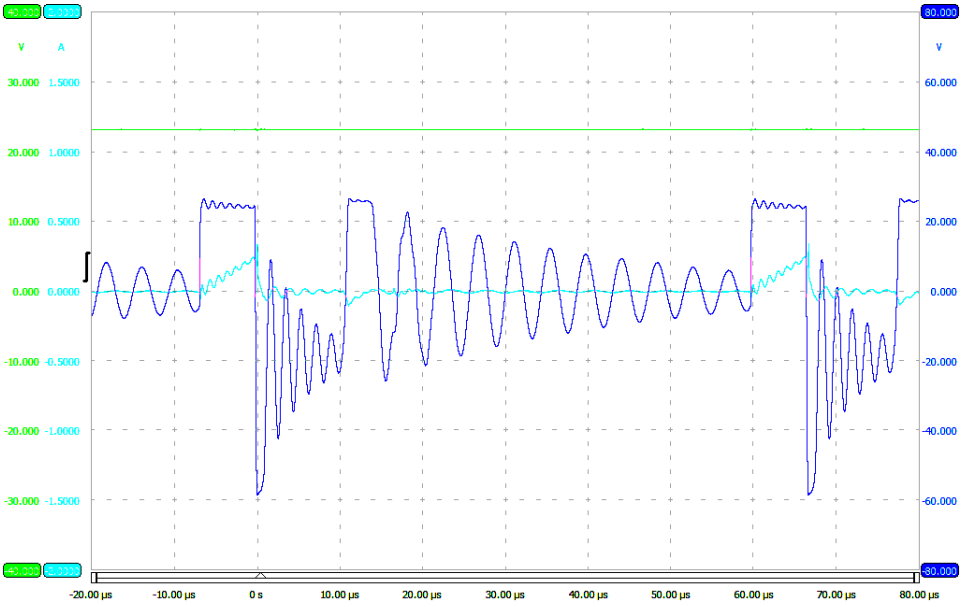

Figure 19: Time-resolved signals at 15 kHz for input voltage (green), current (blue-green) and power (blue), coil 4, with secondary load

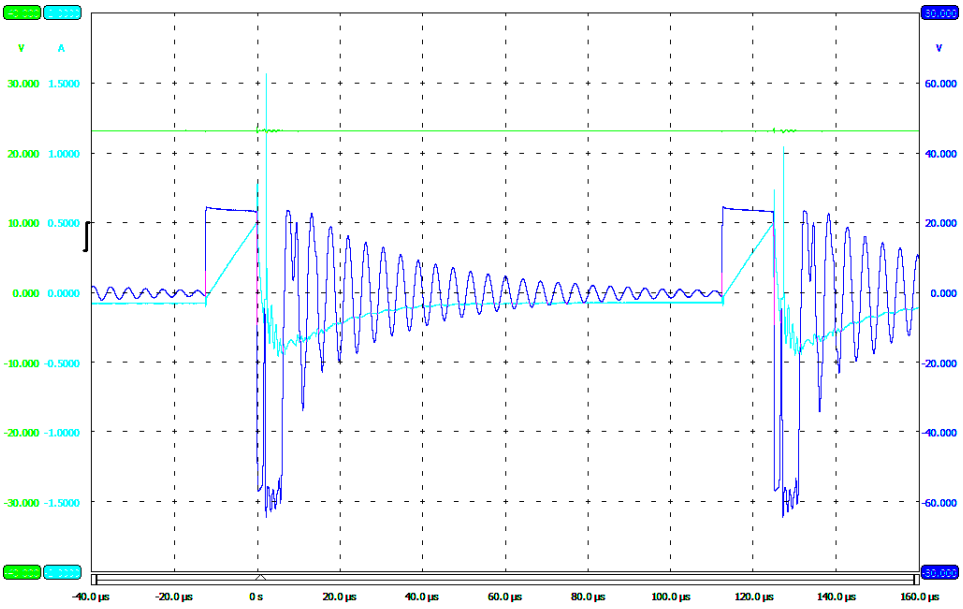

Figure 20: Time-resolved signals at 8 kHz for input voltage (green), current (blue-green) and power (blue), coil 4, with secondary load (cf. with Fig. 19).

3.3 Coil 5

For coil 5 the duty cycle was reduced to 10% to give comparable results as for coil 3 and coil 4. The power curves (Figs. 21, 22) look similar as before, the same does the negative output voltage (Fig. 23).

For this device we also varied the duty cycle in the lower frequency range, resulting in input and output power values as graphed in Fig. 24. The effects can more clearly be seen in the power difference diagram Fig. 25. Highest overunity efficiency is obtained for a small duty cycle of 5%. With decreasing duty cycle, overunity starts at lower frequencies. Tests with the other coils showed that 15% is the optimum value for those devices. The negative output voltage for coil 5 (Fig. 26), however, is lowest for high duty cycles, when considering a fixed frequency. This means that - when considering the output voltage (and load adaptation), - higher duty cycles are better, but considering the overunity behaviour, performance is lower for higher duty cycles. This makes it difficult to find suitable operating points for this type of coil.

The last investigation concerns instabilities in the signals. As an example, the time signal at 57 and 60 kHz is graphed in Figs. 27 and 28. From Fig. 27 it can be seen that nearly two peaks of the eigen oscillation fit into one time interval of the driving frequency. When the frequency is slightly enhanced (57 to 60 kHz), the eigen oscillations start at different time intervals after the duty cycle pulse. These intervals alternate so that the second oscillatory peak only appears in each second period. This seems to be a reason for instabilities in behaviour. The situation has further been analyzed at a low frequency of 15 kHz in Fig. 29. The eigen oscillation completely decays within one period so that there is no instability at low frequencies.

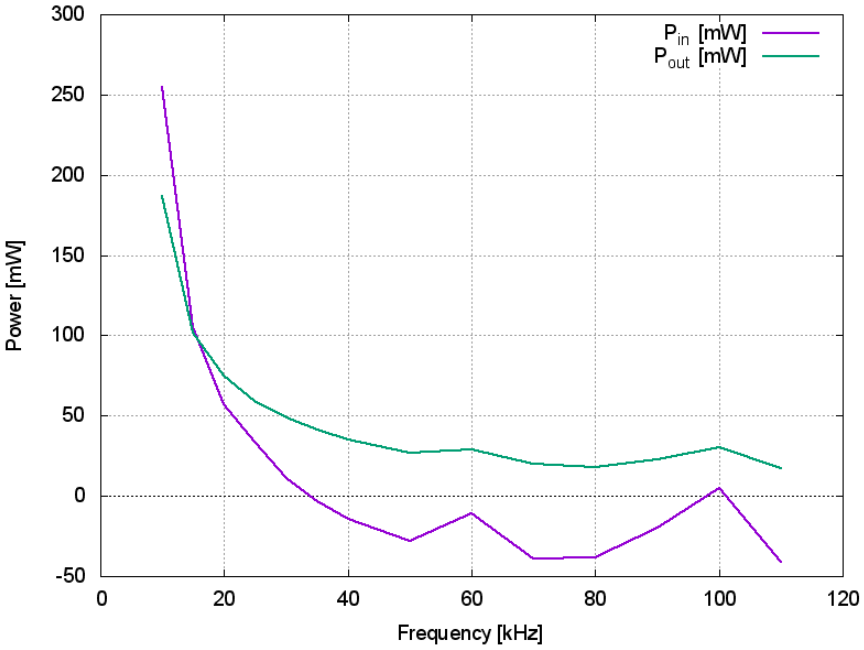

Figure 21: Input and output power of coil 5, neg. half-wave.

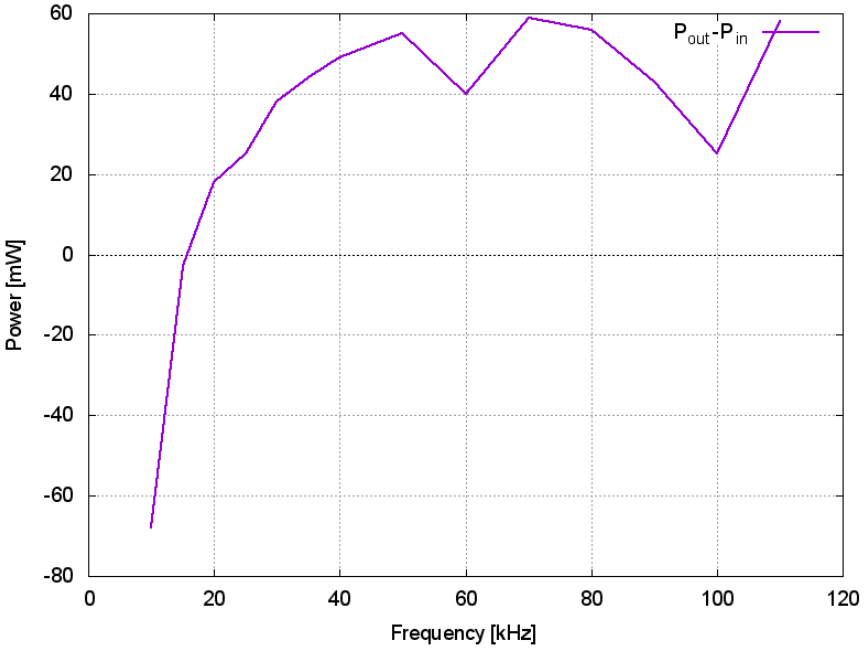

Figure 22: Power differences of coil 5 from Fig. 21.

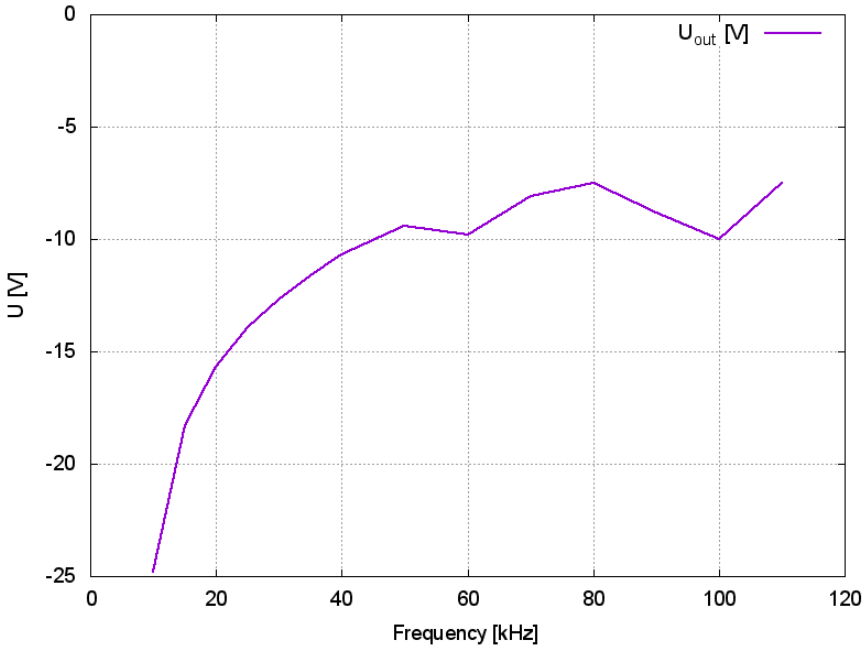

Figure 23: Output voltage (negative rectifier) of coil 5.

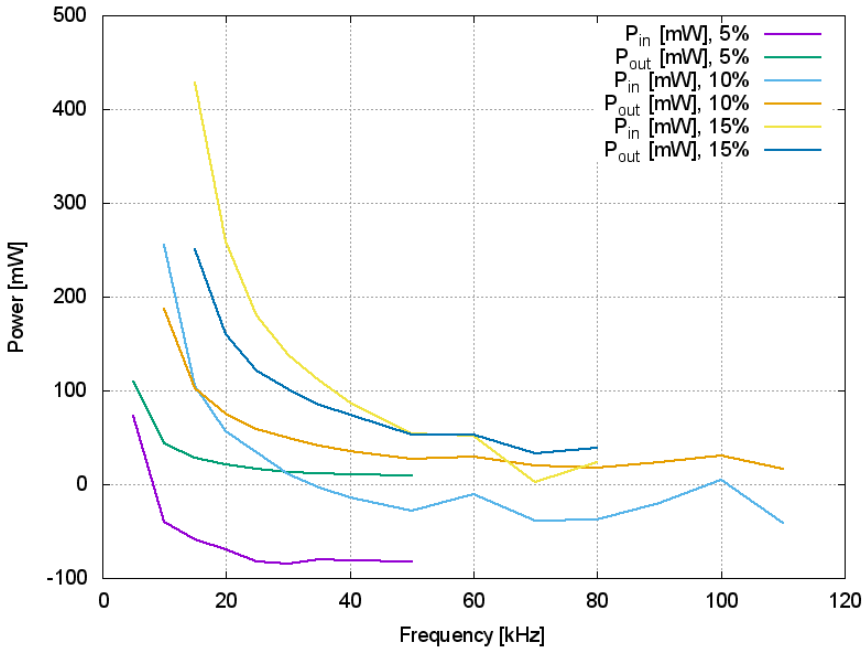

Figure 24: Input and output power for different duty cycles.

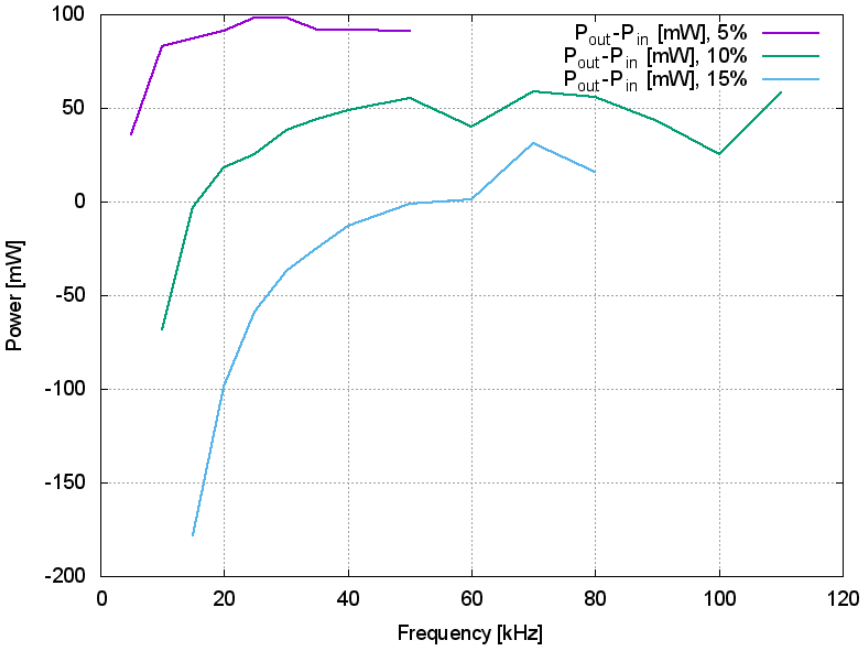

Figure 25: Power differences for different duty cycles.

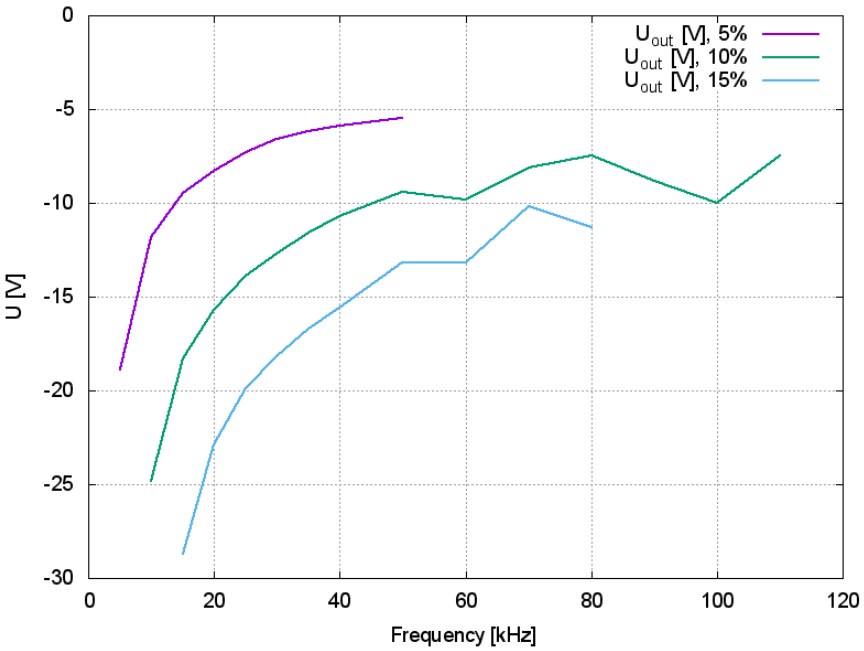

Figure 26: Output voltage (negative rectifier) for different duty cycles.

Figure 27: Instability of coil 5 at 57 kHz, symmetric state.

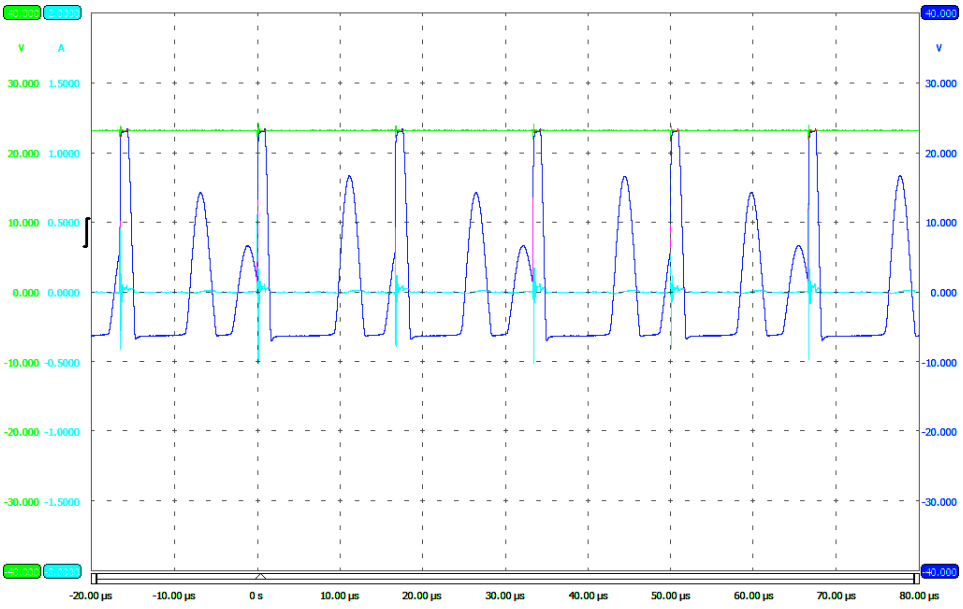

Figure 28: Instability of coil 5 at 60 kHz, alternating state.

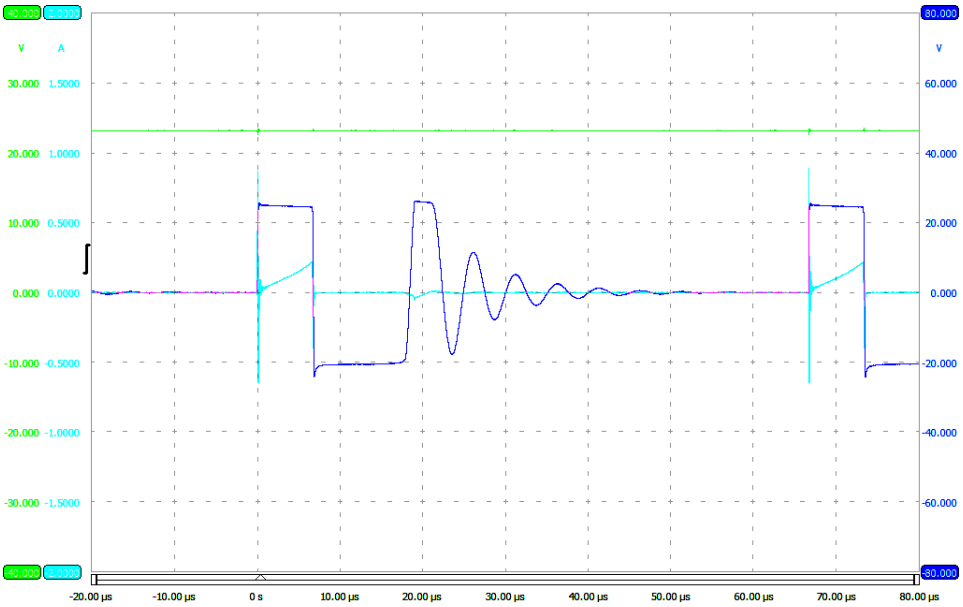

Figure 29: Decay of eigen oscillation at 15 kHz.

4 Summary and discussion

The Ide transformer circuit with rectifiers has been studied with three different types of transformer coils. The decoupling of primary and secondary windings led to a similar behaviour but a frequency shift for onset of overunity power display. A small torus-shaped core required lower duty cycles and was not as well suited for the Ide application as the E-I shaped cores. The Ide device - although being a simple structured circuit - is a complicated high-frequency device and requires special measures of high-frequency engineering for understanding its behaviour. An AC feedback from the secondary side to the primary side improves the overunity behaviour significantly. The input voltage source has to be insensitive to signals acting back to the source from the rectangular signal generator.

A display of negative input power values does not mean that power is re-transmitted to the source but is a special effect of phase shifts. We made additional tests, disconnecting the power source from the circuit during operation. If the negative power would mean a re-transmission of power, the circuit should stay operating, but it did not and dissipated its energy within about a minute. So the negative power display means a special phase relation.

The measured overunity behaviour of Ide's original device with two rectifier paths [3] has been confirmed, with some improvements made in the devices used for this work. A real functional test for the device working as a power generator is still outstanding. Power has to be fed back to the input and the device has to be made self-looping.

References

[1] O. Ide, T. Yamazaki, T. Maeza, T. Funabashi, and H. Ichinose, "Consideration of the Cause of Inverter Noise called Ringing", to be published in Proceedings of the ACS Meeting, Denver, 2015.

[2] O. Ide, T. Yamazaki, T. Maeza, T. Funabashi, and H. Ichinose, "Anomalous Rising of Input Current Induced in the Transformer of Inverter", to be published in Proceedings of the ACS Meeting, Denver, 2015.

[3] O. Ide, "Characteristics of DC Power Output from an Inverter Driven by Sharp Spike Pulse", to be published in Proceedings of the ACS Meeting, Denver, 2015.

[4] K. Arenhold, H. Eckardt, "Experimental verification and theoretical explanation of the Osamu Ide experiment", www.aias.us, UFT paper 311, 2015.

[5] H. Eckardt, D. W. Lindstrom, "Circuit theory for unusual inductor behaviour", www.aias.us, UFT paper 321, 2015.

[6] H. Eckardt, B. Foltz, "Replication of the Ide transformer device", www.aias.us, UFT paper 364, 2016.

[7] M. W. Evans, "Generally Covariant Unified Field Theory" (Abramis, Suffolk, 2005 onwards), volumes one to five, also available on www.aias.us as single articles.

[8] D. W. Lindstrom, "On the Possible Existence of a Second Form of Electrical Current in the ECE Equations of Electromagnetism", www.aias.us, 2008.